Beam-Pointing Optimization for Proton Backlighting on the NIF

Yifan Kong

Webster Schroeder High School

Advisor: **Dr. R. S. Craxton**

Laboratory for Laser Energetics

University of Rochester

Rochester, New York

November 2013

1. Abstract

Optimized designs have been developed for proton backlighting on the National Ignition Facility (NIF) using the hydrodynamics simulation code *SAGE*. In proton backlighting, the deflections of a short pulse of protons are used to measure the electric and magnetic fields in a primary laser-irradiated target. It is proposed to use twenty-four of the NIF's 192 beams (providing 20 kJ of energy) to implode a thin D^3He-filled glass shell 210 μm in radius, generating protons from the reaction $D + {}^3He \rightarrow \alpha + p.$ The remaining beams irradiate the primary target. The optimized design for the selection and aiming of the backlighter drive beams yields an energy deposition uniformity of 9.6% rms, a large improvement upon the 76% of an initial design. A simulation using the hydrodynamics code *DRACO* of a design similar to – but not as uniform as – the optimized design predicted a yield of 2.3×10^{10} protons, well above the required minimum of 10^9. The design calls for the NIF's standard phase plates (which increase the beam spot size) to be removed. An additional design using the phase plates provides more uniformity (7.1% rms); while this design produces a slower implosion, it may still provide an adequate proton source.

2. Introduction

Nuclear fusion has the capacity to supply the future with clean, renewable energy. A virtually inexhaustible source of power, fusion does not harm the environment or contribute toward global warming and relies on fuel found readily in water rather than on oil or gas. One method to achieve nuclear fusion is to use high-powered lasers to irradiate a small (1 to 3 mm in diameter) target consisting of a glass or plastic shell typically surrounding a layer of cryogenic deuterium (*D*) and tritium (*T*).[1] When irradiated, the shell's exterior ablates outward, which causes an opposing force to implode the inner portion of the target. The implosion compresses the cryogenic *DT* layer to an extremely high density and ensures a large number of fusion reactions before the target explodes. The implosion simultaneously heats the fuel to temperatures around 100 million degrees Celsius, which provides the relative kinetic energy needed for the positively charged *D* and *T* nuclei to overcome the Coulomb barrier and fuse together. This fusion reaction results in a helium nucleus and an energetic neutron with the neutron accounting for most of the energy released. The energy of the helium nucleus is deposited in the fuel in a process known as ignition. Ignition makes breakeven possible, which is the point at which energy output equals energy input. Still larger targets will produce one hundred times the amount of energy put in, which would offer laser fusion as a plausible energy source.[2]

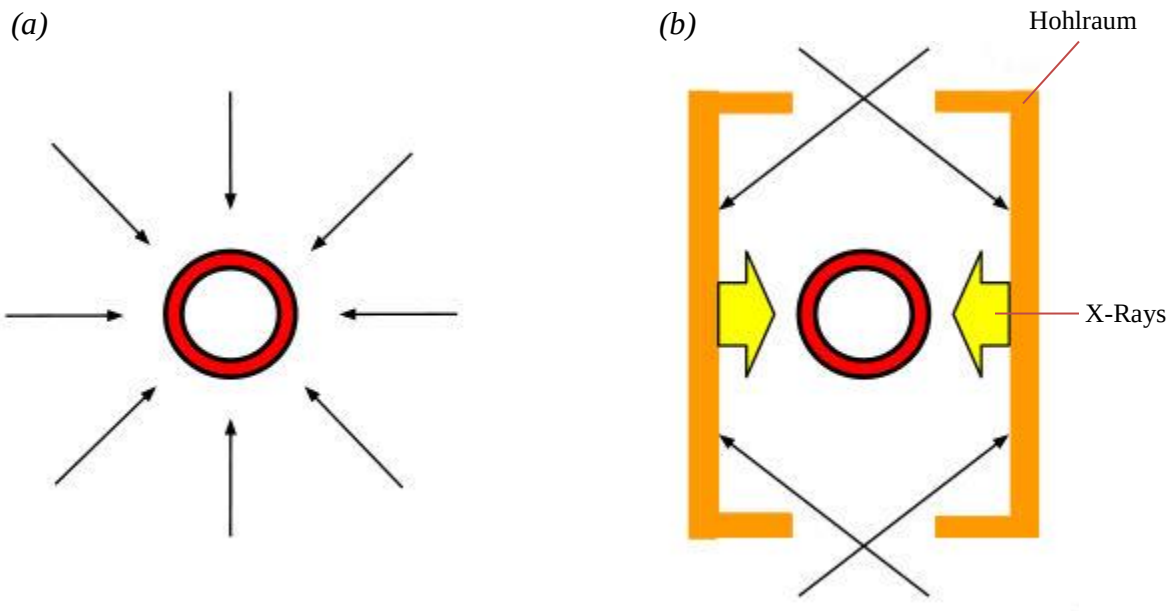

Figure 1: The two main approaches to inertial confinement fusion (ICF). (a) Direct drive calls for laser beams that are aimed directly at the target. (b) Indirect drive calls for beams that strike the inner walls of a cylindrical hohlraum, thereby generating X-rays that then irradiate the target. (Based on Figure 1 of Ref. 3)

Laser fusion can be executed through two chief approaches: direct drive and indirect drive. Direct drive involves positioning each beam around the target to strike the shell directly, usually at normal incidence [Figure 1(a)]; indirect drive involves directing beams through the openings of a metallic hohlraum [Figure 1(b)] to strike the cylinder's inner walls. Once struck, the walls (typically made of gold) emit X-rays that bathe over the target. Proponents of this method argue that indirect drive offers greater uniformity than direct drive. However, there is a significant loss of deposited energy; only 20% of the X-rays are absorbed by the target because the majority of the energy is lost either in the hohlraum walls or through the openings at the ends of the hohlraum.

The National Ignition Facility (NIF) at the Lawrence Livermore National Laboratory is configured for indirect drive and is currently the most powerful laser in the world; with 192 beams bundled in forty-eight quads of four, the NIF can deliver a total energy of 1.8 MJ to a

target. The laser beam ports are arranged into eight equally spaced rings of quads around the target (four quads each in the two rows closest to the north and south poles and eight each in the two rows above and below the equator, shown as black squares in Figure 4 below) and are divided between the northern and southern hemispheres at polar angles (Θ) of 23.5°, 30.0°, 44.5°, and 50.0° to the vertical. To allow for direct drive experiments to be conducted on the NIF, polar drive is used. Polar drive [Figure 2] is a method in which the beams are repointed away from the poles and toward the equatorial region to compensate for the lack of ports near the equator.[4, 5]

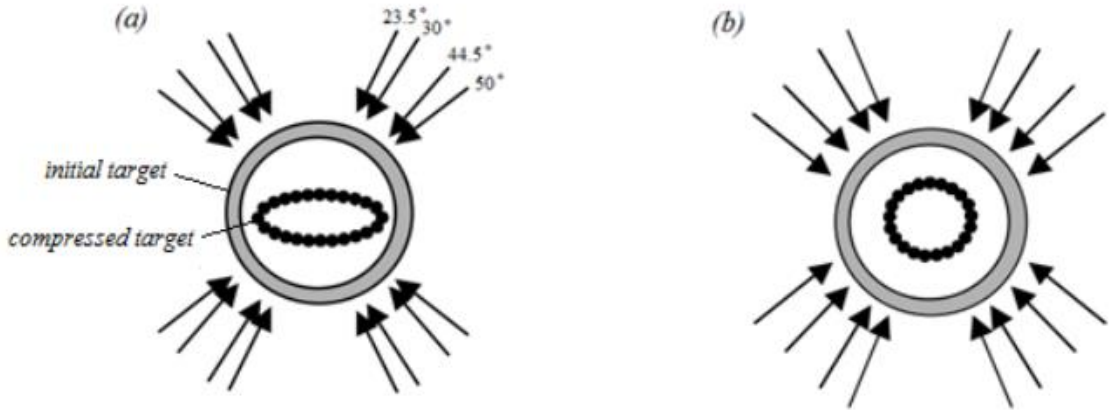

Figure 2: Direct drive without repointings versus polar drive on the NIF (Figure 3 of Ref 3). (a) Pointing the laser beams directly at the center of the target results in very poor uniformity of the compressed target. (b) Using polar drive, shifting the beams towards the equator allows for maximum implosion uniformity.

Another use for direct drive implosions is proton backlighting.[6] Proton backlighting uses protons generated by a backlighter target to probe a primary target. Figure 3 shows the setup, which involves a backlighter and a primary target. Because there are two targets, two different sets of beams must individually irradiate each target. Protons are released through the implosion of the backlighter from the reaction $D + {}^{3}He \rightarrow \alpha + p$. They have an energy of 14.7 MeV and pass through a mesh that organizes the protons into separate beamlets. An image is projected

onto a surface (in Figure 3's case, a piece of CR-39 plastic, shown in green) after the backlighter protons are deflected as they pass through the plasma produced by the main target implosion. An image can also be produced through proton absorption rather than proton deflection in which areas of higher density in the main target absorb more protons so that the excess protons strike the screen and outline the shape of the implosion.

Dr. Chikang Li of the Massachusetts Institute of Technology's Plasma Science and Fusion Center has proposed a larger-scale monoenergetic proton backlighting experiment for the NIF using proton deflection to measure the electric and magnetic fields in laser-produced plasmas. In the proposed experiment, the backlighter is a target measuring 210 μm in radius filled with D^3He fuel encapsulated by a thin (2 μm thick) glass shell. This experiment calls for a direct drive implosion of the proton backlighter using polar drive. However, because the experiment only allows six of the possible forty-eight quads to be reserved as backlighter drive beams, polar drive is made considerably more difficult. The best combination of six among the possible forty-eight quads must therefore be determined.

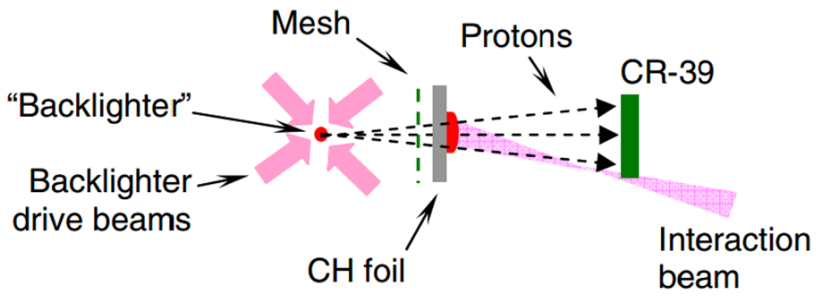

Figure 3: Setup for a proton backlighting experiment conducted by Dr. Chikang Li on the OMEGA Laser at the University of Rochester's Laboratory for Laser Energetics (Ref 6). The setup involves a backlighter and a primary target (in this case, a CH foil), which prompts the use of two different sets of beams to individually irradiate each target. An image is projected onto a piece of CR-39 plastic (shown in green) after the backlighter protons are deflected as they pass through the plasma produced at the interaction beam-CH foil interface.

The proposed experiment begins with the interaction beams irradiating the main target. The backlighter drive beams (consisting of 24 of the possible 192 NIF beams delivering 20 kJ in combined laser energy at a steady rate over 400 ps) then use polar drive to implode the proton backlighter, causing a short burst of protons. To produce a clear image, at least 10^9 protons must be produced by the implosion. These protons pass through a mesh and are (depending on the imaging technique) either deflected by electric and magnetic fields or absorbed by the main target before striking a screen to produce an image.[7]

The present work involves the selection of six quads and the optimization of the pointings of the 24 selected beams to implode the proton backlighter as uniformly as possible. There were three main stages of design, the first being the examination of an initial design[8] which proved to yield poor uniformity. The second stage involved designs based on geometric solids. These produced an improved uniformity, but were not optimum. The third stage was the final development of an optimized design. Once the optimization process was complete, another optimized design was developed that kept the NIF's phase plates in place (rather than remove them for the experiment). However, because of the resultant decrease in energy deposited on the target surface, the phase plate design may not produce enough protons to clearly image an imploding target. One application of proton backlighting to diagnose polar drive implosions was also considered.

3. Initial Design

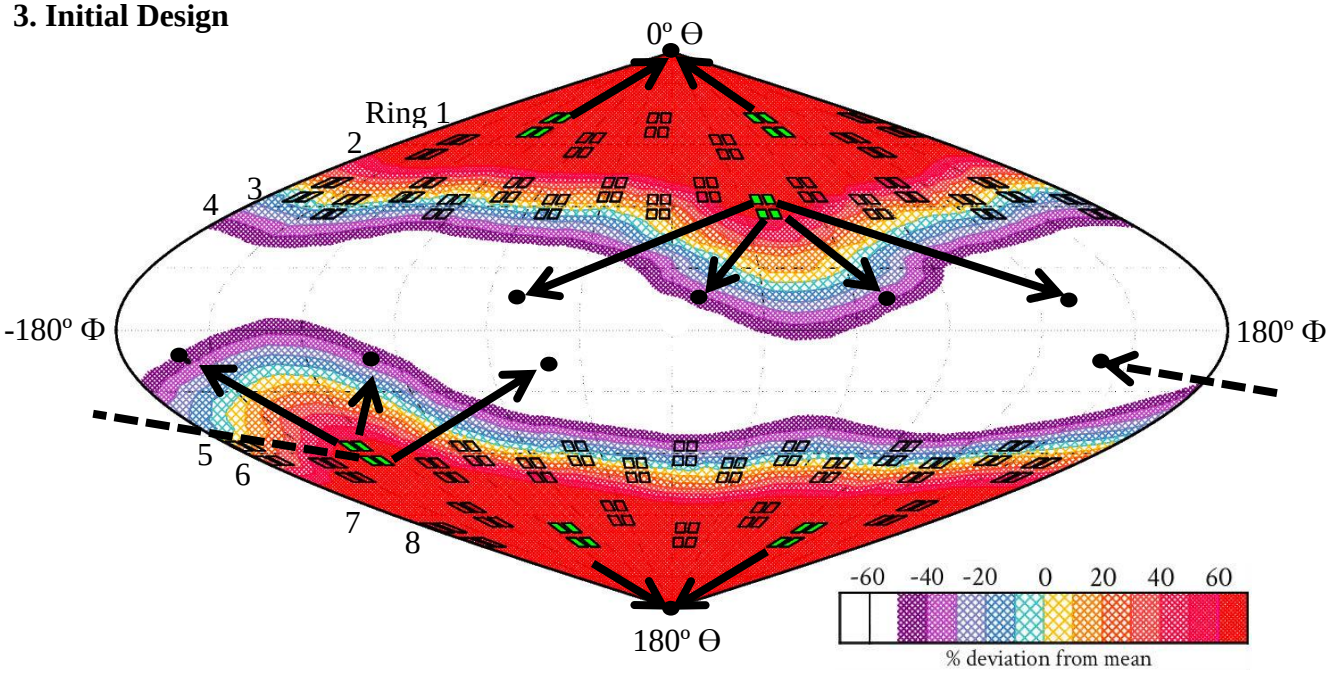

Figure 4: Energy deposition contours on a sinusoidal projection for the initial design 200 ps after the backlighter drive beams were turned on. The groups of four black squares (beams) indicate where the quads are positioned in the target chamber in relation to the target; quads highlighted in green are the ones selected for the design. The beam repointings are indicated by the arrows pointing to black dots, eight of which fall in the equatorial region, eight on the south pole, and eight on the north pole (the pointings clustered at the poles overlap, so only a single dot is shown).The rings (rows of quads) are numbered down the left-hand side

As shown in Figure 4, the initial design's quads were arranged so that four of the six quads chosen lay in the rings closest to the poles (ring 1 in the north and ring 8 in the south) with all four beams in each of these quads pointed at the closest pole. This left only two quads in rings 4 and 5 to spread their beams along the equator.

The colors of the contours used in Figure 4 indicate the percent deviation from the average amount of energy deposited on the surface calculated using the two-dimensional hydrodynamics code *SAGE*. Colorless areas denote portions of the target that received minimal amounts of energy (less than 50% of the average) while red areas connote portions that received maximum amounts of energy (over 60% of the average). The initial design yielded an rms (root mean square) energy deposition value of 75.5%. Rms is a measure of deviation; thus, to ensure a

uniform implosion, the value of the rms needs to be as low as possible. The lack of uniformity is due mostly to the poor choice of quads and beam pointings, which caused a large disconnect between the maximum and minimum amounts of energy deposited.

Because the NIF is designed for indirect drive experiments, the energy deposited by the beams is concentrated at the poles by default. Thus, the primary goal should be to redirect the energy to the equator. However, the initial design called for the majority of the quads and beams to be located on and around the poles, which explains why the poles receive most of the deposited energy (the maximum amount of energy deposited being 170% of the mean) and the equator was left strongly underdriven (the minimum being 94% under the mean).

The poles are propelled toward the center of the target with a greater velocity than the equator due to the disproportionate amount of energy concentrated at the top and bottom. This will cause the poles to collide first at ~200 ps [Figure 5(a)] before the equator collides at ~400 ps [Figure 5(b)]. Such an implosion is not desired because uniformity is needed to maximize the proton yield and to ensure that the protons are produced in the shortest time interval possible.

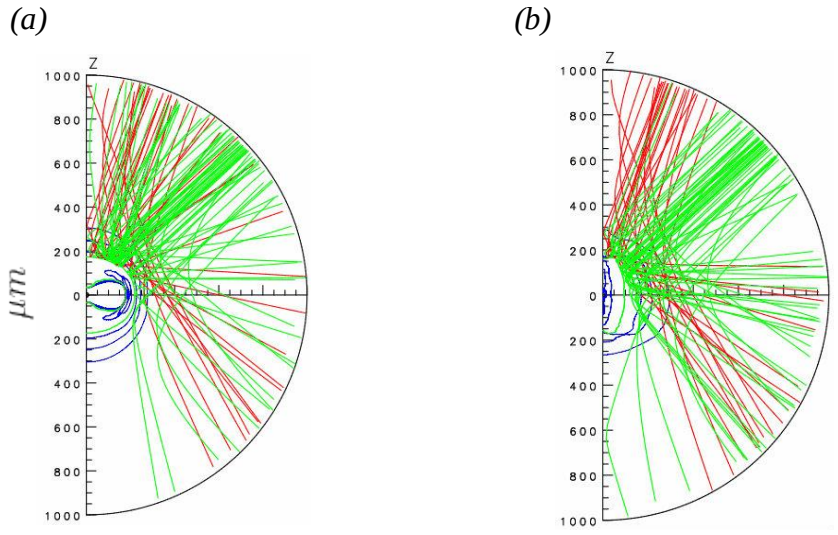

Figure 5: Ray-trace diagrams of the initial design with two incoming beams shown in red and green. The blue lines indicate the density contours of the target. (a) At ~200 ps, the poles collide while the equator has moved little from its initial radius of 210 μm. (b) At ~400 ps, the equator collides as the poles are already exploding back outwards.

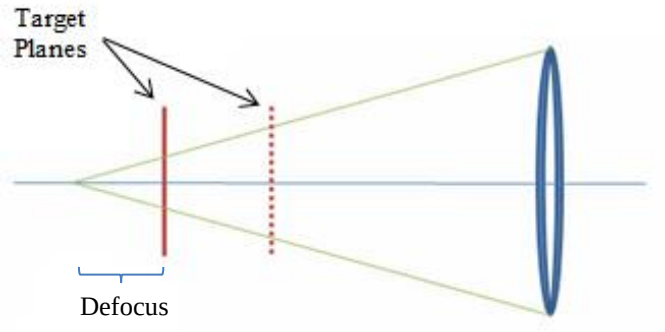

Figure 6: Defocus is the distance between the target plane and the point of best focus (where the rays converge). Increasing the defocus increases the size of the beam spot on the target plane; for example, the dotted target plane is covered by more of the rays than the solid target plane because its defocus is larger.

To improve the initial design, *SAGE* was used to optimize three main experimental parameters: quad selection, beam pointing, and defocus. Individual beams were able to be repointed to new polar (Θ) and azimuthal (Φ) angles and were set to beam-specific defocus distances [Figure 6]. By adjusting the pointings of each of the twenty-four beams prescribed for the experiment, more or less energy can be distributed to certain points on the target surface, enabling the shape of the imploding target to be manipulated. In order to compare different designs, different facets of each run needed to be taken into account (i.e., the rms energy deposition just before implosion and the total energy absorbed). Energy absorption is an important consideration in that enough of the 20 kJ of incident energy provided by the twenty-four backlighter drive beams needs to be deposited and absorbed by the target in order to yield a fast implosion, a high temperature during implosion, and a high proton yield.

4. Designs Based on Geometric Solids

Having noted the problems with the initial design, new designs were produced. The first designs in the optimization process were based on geometric solids with equally spaced vertices. The first configuration was derived from an inscribed octahedron in that each of the six quads chosen for the design was pointed at one of six equidistant vertices. This design [Figure 7] produced an rms of 24.7%. It imploded at 250 ps, which occurred later than the initial design's

implosion because the improved uniformity ensured that the poles would not collide with a much greater velocity than the equator. Although each quad consists of four beams with independent repointing capabilities, the first design kept each quad bundled to a single aim point in order to produce a result that would indicate where energy needed to be mitigated.

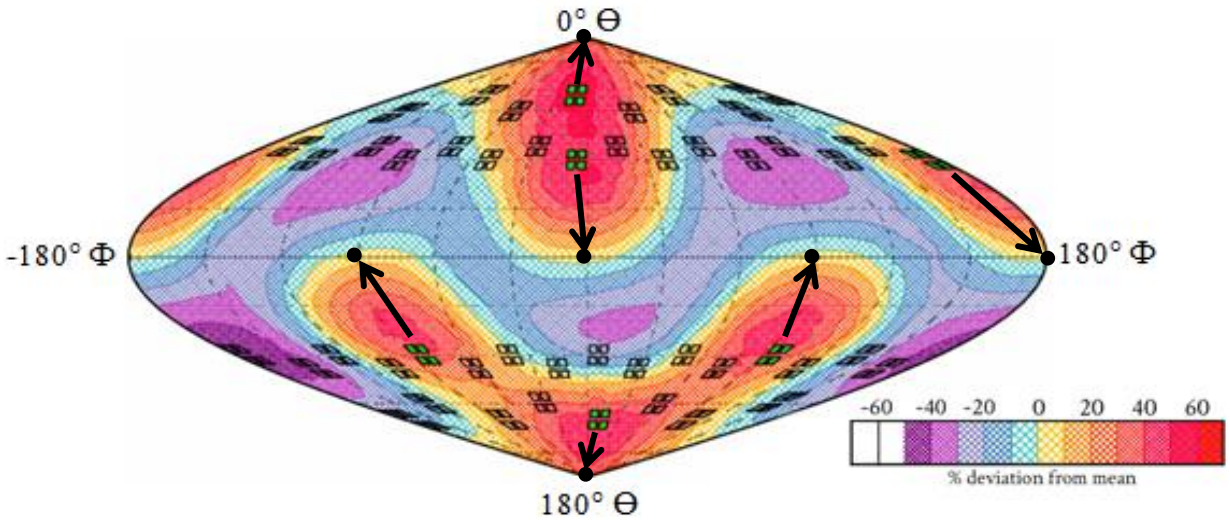

Figure 7: Energy deposition profile for an octahedral design 250 ps after the drive beams were turned on. Each quad in green is pointed at one vertex of an octahedron.

As can be seen in Figure 7, the areas of high deposition coincide with the quad selection. Essentially, the energy a quad deposits is concentrated around its place of origin in an "area of influence," and repointing beams only serves to shift the entire area toward a certain direction while the area is still anchored to the placement of its original quad. For example, quad [R5, 7], the quad in Ring 5 (see Figure 4) and 7 quads to the right of Φ = 0° (3 quads to the right of Φ = -180°), is pointed at (0, 270º), but the majority of its deposited energy lies not even halfway between the location of the quad and its aim point. The problem with quads' areas of influence is a major issue in that as much energy as possible needs to be funneled toward the equator, but large repointings lower the amount of energy deposited and do not redirect energy far enough from the quad of origin. Another problem is the inherent asymmetry of the design. Because the

design calls for six quads, three quads must be arranged in a symmetrical fashion in each of the northern and southern hemispheres. Furthermore, the chosen quads should lie as close to the equator as possible in order to concentrate as much energy as possible in that region.

The second design was based on an inscribed rhombicuboctahedron (RCO), which has twenty-four equidistant vertices, but with all aim points shifted toward the equator in order to divert more energy along the central band.

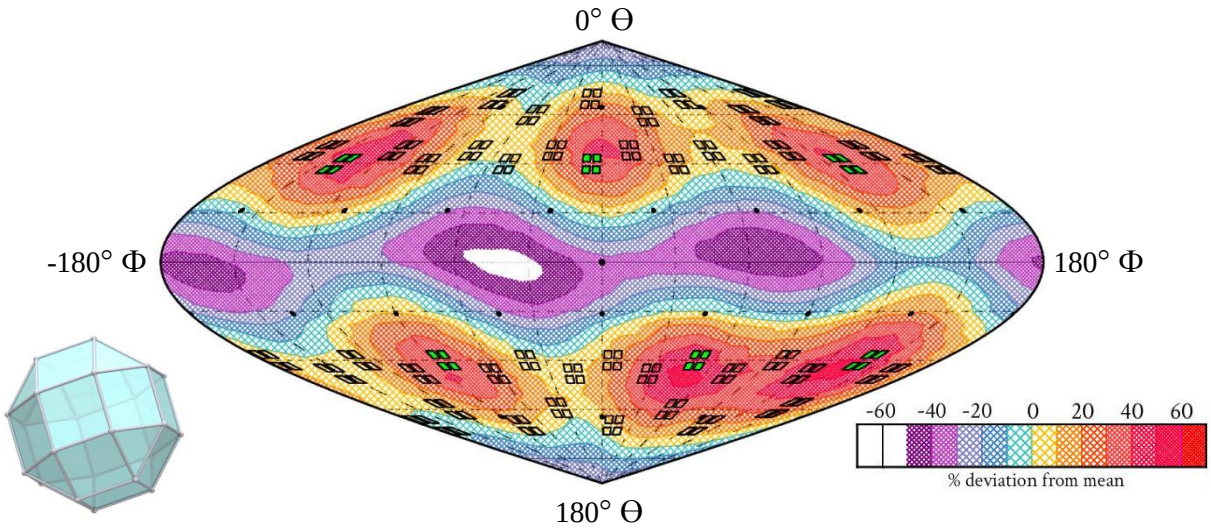

Figure 8: Energy deposition profile for a rhombicuboctahedral design 250 ps after the drive beams were turned on. The blue image is of a rhombicuboctahedron (Ref 9).

Each of the twenty-four beams allotted for this experiment was pointed near a vertex of an RCO and all quads used were chosen from rings 4 and 5. However, because these rings each contain eight equally spaced quads, it is impossible to choose three of the possible eight and maintain perfect symmetry. As a result, no matter the quad set-up chosen, there will always be abnormalities in a few sections (e.g., the white spot along the equator in Figure 8). The increased beam dispersion aided the spreading of energy and improved the uniformity of the implosion to an rms of 25.4%.

5. Optimized Design

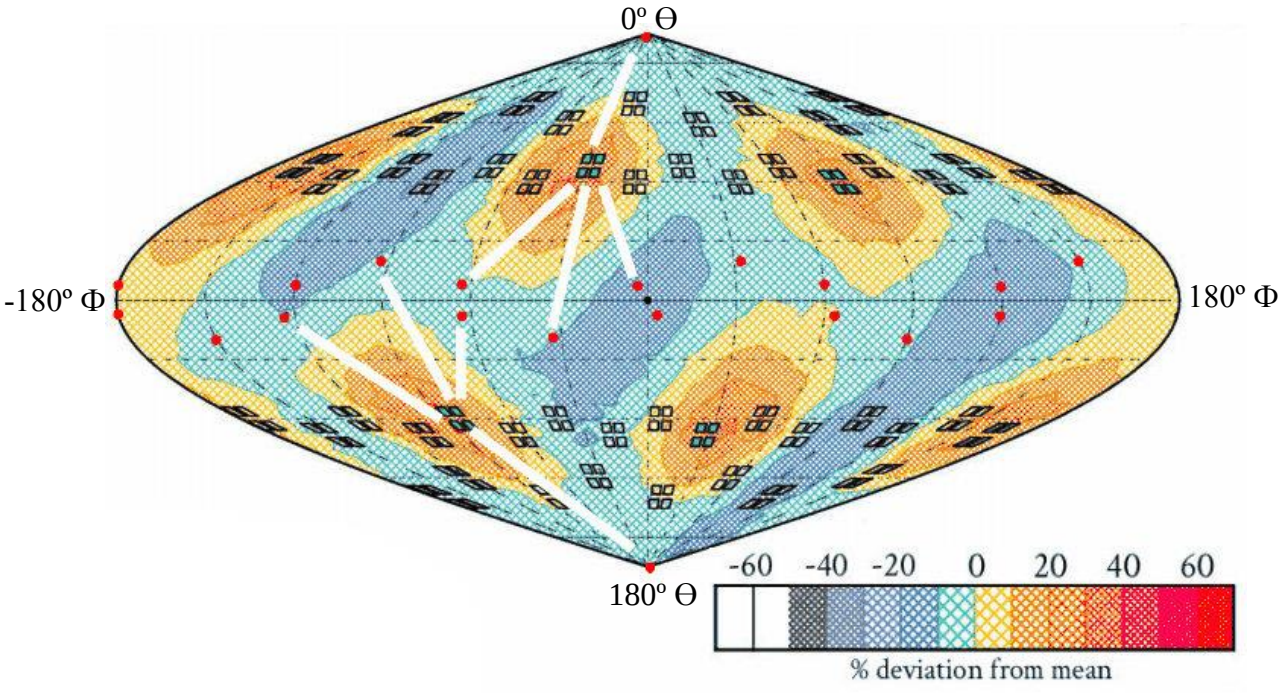

Figure 9: Optimized design. For each quad, three beams were pointed toward the equator and one toward the pole. Red spots indicate aim points; the poles each have three beams redirected there and are indicated by a single red dot. The white lines indicate beam repointings. Because the repointing pattern repeats at regular intervals, only two quads are shown with repointings.

The optimized design is illustrated in Figure 9. All quads were selected from the rings closest to the equator and for each quad, three beams were pointed toward the equator and one toward the closest pole. The design yielded a 9.6% rms, decreasing the original 75.5% by a factor of about seven. Based on a similar design with an 11.1% rms that was modeled using the two-dimensional hydrodynamics code *DRACO*,[8] it can be assumed that the optimized design will produce at least 2.3×10^{10} protons, comfortably exceeding the 10^9 goal.

In reducing the rms to obtain the most uniform implosion possible, a few glaring problems needed to be addressed. First, the defocus (the distance between the target plane and the point of best focus, see Figure 6) and amount of deposited energy are inversely related. For

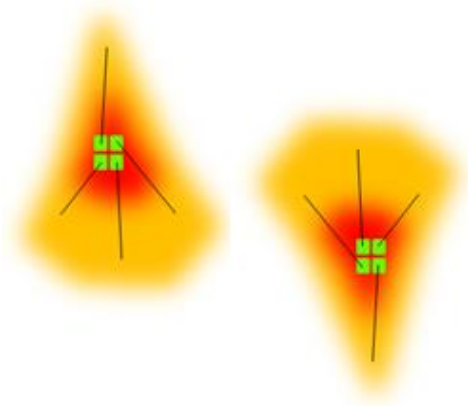

Figure 10: Three-to-1 separation of beams in a quad (a grouping of four green rectangles). The black lines show where each beam (one green rectangle) has been repointed to and areas in red show more energy deposition than orange areas. This method proved most effective in directing as much energy as possible toward the equator without completely neglecting the pole. It also diffused the concentrated deposition of energy centered around each quad in use, which increased uniformity.

this reason, there is a point where increasing the defocus lowers the energy deposited by an excessive amount (the amount of energy deposited should remain high in order to ensure a larger proton yield). Second, beam repointing can only fine-tune the areas of deposited energy decided by quad selection. To maximize the benefits of beam pointing, a 3:1 ratio was used in separating a quad's four beams into two subsets directed at different regions of the target [Figure 10]. Using this method, one beam was sent to its hemispherical pole while the remaining three were sent toward the equator with the middle beam repointed a bit further than the others. This method allowed the majority of a quad's energy to be shifted toward the equator without neglecting the pole entirely.

To reduce the effects of asymmetry, the three quads used in each hemisphere were staggered between the two rows closest to the equator. This allowed the three chosen quads to be spaced at more even intervals. With this method, however, it was extremely important to mirror the northern and southern hemispherical quad placements. For example, since quad [R3, 8] was selected, quad [R6, 1] was also chosen because they are equidistant from the equator and are reflections across the $\Phi = 0°$ axis. This also created a staggering effect in that between any two used quads in one hemisphere, there would be a used quad in the other hemisphere. In so doing, areas of high energy deposition were staggered north-south-north-south of the equator, which

aided the symmetry of the design as well as the uniformity. Furthermore, quads were chosen only from the four rows closest to the equator, which focused more energy around the equator.

In Table 1, the main parameters for optimization were the quad choice, the Θ and Φ of each beam's aim point on the initial target, and the defocus of each beam.

Quad	NIF Beam No.	Θ (deg)	Φ (deg)	Defocus (cm)	Quad	NIF Beam No.	Θ (deg)	Φ (deg)	Defocus (cm)
R3, 5	41	85.0	180.0	0.70	R5, 7	109	77.0	267.0	0.82
	42	0.0	0.0	0.70		110	95.0	297.0	0.82
	57	103.0	210.0	0.82		125	95.0	237.0	0.70
	58	85.0	240.0	0.82		126	180.0	0.0	0.70
R3, 8	47	85.0	297.0	0.70	R6, 1	129	95.0	3.0	0.82
	48	0.0	0.0	0.70		130	77.0	33.0	0.82
	63	103.0	327.0	0.82		145	180.0	0.0	0.70
	64	85.0	357.0	0.82		146	95.0	63.0	0.70
R4, 2	67	0.0	0.0	0.82	R6, 4	135	95.0	120.0	0.82
	68	85.0	120.0	0.82		136	77.0	150.0	0.82
	83	85.0	60.0	0.82		151	180.0	0.0	0.82
	84	103.0	90.0	0.82		152	95.0	180.0	0.82

Table 1: Beam parameter specifications for the six quads used in the optimized design. [R3,5] denotes Ring 3 (Ring 1 being the topmost ring), 5 quads to the right of Φ = 0°. Beams are numbered by rings of constant latitude counting from the top and increasing with Φ within each ring.

6. Optimized Design Using Phase Plates

Phase plates are large optics installed on the NIF that spread the energy deposited by beams over a larger area [Figure 11(a)]. They consist of a glass substrate with small random nonuniformities polished onto one surface to deflect incoming laser rays. The NIF uses these optics to avoid excessive intensity when the beams are focused at a laser entrance hole in the hohlraum [Figure 1(b)].

Because they are inconvenient to remove, a natural question to ask is whether or not a design can be developed without having to remove the NIF's phase plates. The major hurdle is

the fact that phase plates cause the beam spot size to become much larger than the target [Figure 11(b)].

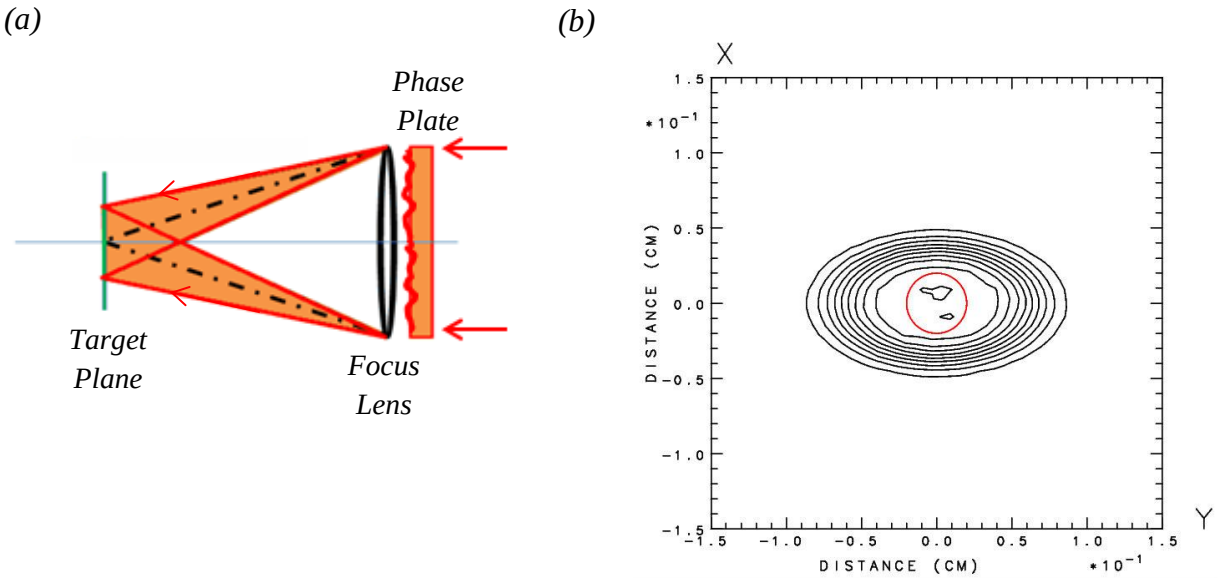

Figure 11: The effect of a phase plate on beam spot size. (a) Beam rays passing through a phase plate. With the phase plates, the original laser rays (the dotted black lines) are dispersed (the orange area around the dotted black lines) and cover more area on the target plane. (b) Intensity contours in the target plane for a typical phase plate. The red circle denotes the size of the target (210 µm in radius) in relation to the beam spot. Thus, the majority of the beam energy completely misses the target.

The phase plates used on the NIF cause the beam spots to become elliptical in shape; for example, the (a,b) for the ellipse in rows 3 and 6 are (635, 367) µm and rows 4 and 5 have an (a,b) of (593, 343) µm. The more uniform dispersal resulting from the large phase plate spots lowers the rms to 7.1%, but it also means that a large portion of energy misses the target completely [Figure 11(b)]. Because less energy is being provided to the target, the target implodes at a slower speed. This can be seen in Figure 12, a plot of electron number density n_e vs. radius at a time of 350 ps, when n_e reaches its peak value at a radius near zero. This implosion takes ~100 ps longer to occur than the optimized design of Section 5. This slowed implosion results from lower temperatures in the target and is expected to produce less protons in

a longer period of time. However, the yield of protons may still be sufficient to produce a clear image.

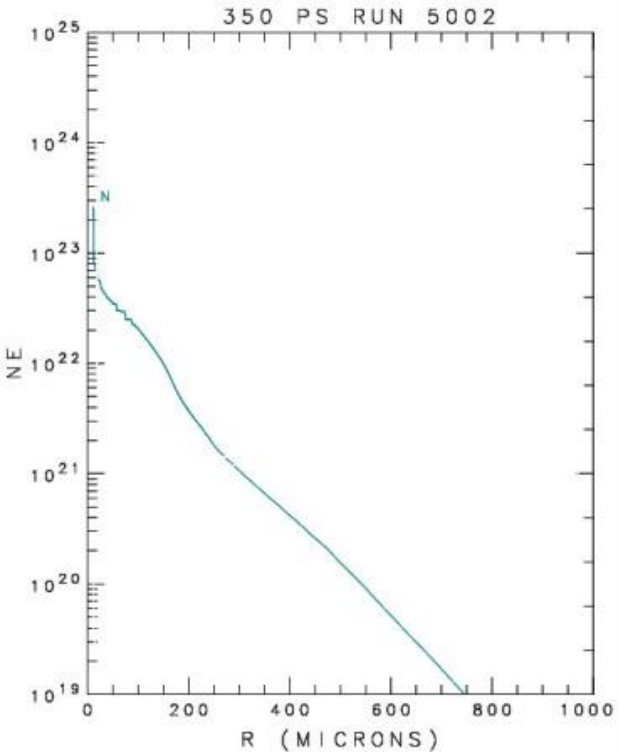

Figure 12: Plot of target electron number density (n_e in units of cm^{-3}) over a period of 350 ps with a phase plate. The implosion occurs at this time as n_e reaches its peak as the radius nears zero.

7. Future Applications

Proton backlighting on the NIF has a number of potential applications. The main target can be a flat target as in Figure 3, a hohlraum, or a polar drive target. Tucker[10] and Olson[3] have developed an optimized polar-drive design using 24 quads. As shown in Figure 13, this design could be used to irradiate the direct-drive capsule with drive beams while the design presented in this paper could be used to generate the protons from the backlighter. Furthermore, if more quads were allotted as backlighter drive beams and phase plates were used, uniformity and the amount of energy absorbed by the backlighter would increase.

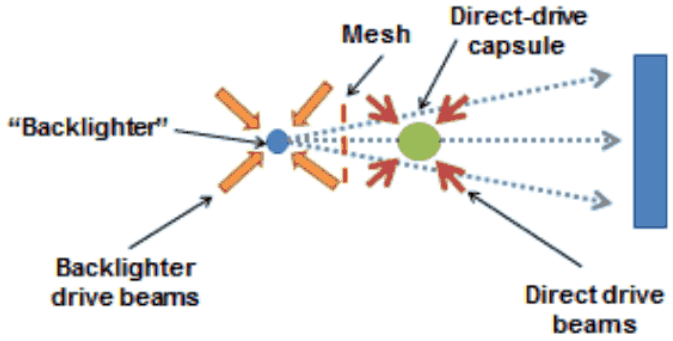

Figure 13: A possible proton backlighting set up to image a direct-drive capsule. As the capsule implodes, areas of higher density will absorb more protons and thus produce an image that can determine how uniform the implosion was based on its shape.

8. Conclusion

Designs have been developed for proton backlighting on the National Ignition Facility (NIF) using the hydrodynamics simulation code *SAGE*. The optimized design for irradiating a proton backlighter using 24 beams yields an energy deposition uniformity of 9.6% rms and over 2.3×10^{10} protons, well above the required minimum of 10^9. Because the design calls for the NIF's standard phase plates to be removed, an additional design using the phase plates was developed to avoid the task of removing the large optics. The phase plate design yields an energy deposition uniformity of 7.1% rms, but less absorption and a slower implosion lead to a lower proton yield. More simulations need to be run in order to determine whether the optimized phase plate design provides a sufficient amount of protons.

9. Acknowledgments

This project could not have been completed without Dr. Craxton, whose consistent advice, feedback, and ready support served as an unwavering guide throughout the entire process. I would also like to thank Tricia Olson for answering my questions and getting me

acquainted with *SAGE*, Dr. Enck for being the first to kindle my interest in physics and in encouraging me to apply for this internship, Dr. Chikang Li for helpful discussions, and Dr. Pat McKenty for the *DRACO* simulation. Lastly, I would like to thank the Laboratory for Laser Energetics for running the summer high school program; it has been an invaluable learning and growing experience.

References

[1] J. Nuckolls et al., "*Laser Compression of Matter to Super-High Densities: Thermonuclear (CTR) Applications*," Nature **239**, 139 (1972).

[2] Stefano Atzeni and Jürgen Meyer-ter-vehn, "*The Physics of Inertial Fusion: Beam Plasma Interaction, Hydrodynamics, Hot Dense Matter*." Oxford: Oxford UP, 2004.

[3] Patricia Olson, "*Optimization of Beam Configurations for Shock Ignition Experiments on the NIF and OMEGA*," Laboratory for Laser Energetics High School Summer Research Program (2011).

[4] S. Skupsky et al., "*Polar Direct Drive on the National Ignition Facility*," Phys. Plasmas **11**, 2763 (2004).

[5] A. M. Cok et al., "*Polar-Drive Designs for Optimizing Proton Neutron Yields on the National Ignition Facility*," Phys. Plasmas **15**, 082705 (2008).

[6] C. K. Li et al., "*Measuring* E *and* B *Fields in Laser-Produced Plasmas with Monoenergetic Proton Radiography*," PRL **97**, 135003 (2006).

[7] C. K. Li, et al., "*Mononoenergetic-Proton Radiography Measurements of Implosion Dynamics in Direct-Drive Inertial-Confinement Fusion*," PRL **100**, 225001 (2008).

[8] Dr. P. McKenty, unpublished

[9] Rhombicuboctahedron [Digital Image]. (2007). Retrieved November 5, 2013, from: http://simplydifferently.org/Geodesic_Polyhedra?page=7

[10] L. Tucker, "A Design for a Shock Ignition Experiment on the NIF Including 3-D Effects," Laboratory for Laser Energetics High School Summer Research Program (2010).